Practical Considerations in Application of Correlation-Based Islanding Detection with Synchrophasors

M. Ropp, S. Perlenfein, D. Schutz, C. Mouw
Northern Plains Power Technologies
Brookings, SD USA
michael.ropp@northernplainspower.com

S. Gonzalez, J. Neely
Sandia National Laboratories
Albuquerque, NM USA

M. Mills-Price
Advanced Energy Industries
Bend, OR USA

***Abstract*—The correlation coefficient-based (CCB) method of islanding detection has been shown to be highly effective in detecting islands in electric power systems. However, due to the high sensitivity of the method, a number of questions remain regarding its practical applicability. In this paper, three such issues are addressed: immunity of the method to false trips during system-level events, sensitivity of the method to time slips in the data, and the question of how large of an area can be covered by a single reference PMU.**

***Index Terms*—Distributed power generation, unintentional islanding, synchrophasors, statistical methods.**

I. Introduction

Most inverters used today for interfacing distributed energy resources (DERs) to distribution systems utilize some form of active detection of unintentional islands. There are many methods available [1,2], with the most effective ones using a combination of impedance detection and positive feedback that destabilizes any unintentional island. These methods are necessary to maintain compliance with IEEE 1547 interconnection requirements which require DERs to cease energizing the power system within 2 seconds of utility disconnect [3]. These methods are highly effective for individual inverters and low penetration levels, but other circumstances can be challenging. Examples:

- Active anti-islanding may interfere with grid support functions (GSFs), or vice-versa.
- When there are both inverters and rotating machines, islanding detection effectiveness can be significantly reduced.
- On low-inertia grids, the destabilizing impacts of active anti-islanding may place an upper limit on the system's DER hosting capacity.

There is thus a need for islanding detection methods that retain a high degree of effectiveness in detecting islands, for any combination or penetration level of DER, while facilitating GSFs. Communications-based methods can meet this need.

Recently, communications-based islanding detection using synchrophasor data has attracted considerable attention. Several methods for using synchrophasor data to detect islanding have been proposed [4-7]. One such method is the correlation coefficient based (CCB) method, in which statistical correlation between local and remote frequency measurements is used to detect islands [5]. This method has been extensively tested in simulation, laboratory and field, so that its islanding detection effectiveness is becoming relatively well-quantified [5,8]. The purpose of this paper is to probe some additional practical aspects of this method, including:

- Immunity to false trips during local or system-level events
- Sensitivity to time slips between the incoming PMU data streams
- Impact of electrical distance between the phasor measurement units (PMUs), and a discussion of how this impacts how large of an area can be covered by a single reference PMU.

II. Description of the CCB

A system used for implementing synchrophasor-based islanding detection is depicted in Figure 1.

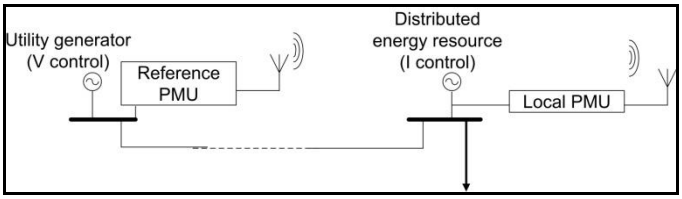

Figure 1. Diagram illustrating the application of PMUs for islanding detection.

A reference, or remote, PMU is located at an upstream point on the system, outside of the potential island. A local PMU is collocated with the DER, inside the island. The reference PMU's synchrophasor data are broadcast to all DER sites (a microwave link is shown in Figure 1). Once received at the DER site, the local and reference PMU data are time-aligned, and then compared in some way to

determine whether the two PMUs are still in interconnected systems. Different synchrophasor-based islanding detection systems are distinguished by the types of comparisons they perform on the data.

In the CCB method, a statistical correlation is calculated between the local and reference frequencies. Several different correlations have been tested, but the most-used one is Pearson's sample correlation coefficient, denoted by r [9]. The concept is simple: if the two PMUs are still in electrically-connected systems, their frequencies should remain well correlated, and r should remain close to 1. When an island is formed, the correlation will drop, ideally to zero. Thus, what is needed is to set a minimum allowable threshold on correlation or a time-threshold pair, and violation of this criterion indicates an island. For the work described here, the trip threshold is set to 0.7, and the time to trip is zero.

The primary strength of the CCB method is that it is expected not to have a nondetection zone (NDZ) in the sense that, for any combination of generation or loads and any level of precise matching, once the island is formed the grid and island frequency controls are independent and the reference-local frequency correlation will drop. Thus, indefinite or sustained run-ons are not expected under any condition. The primary weakness of the CCB is that in certain cases it can be slow to detect an island. It has been observed that under specific conditions of island generation-load mismatch, the remote-local correlation initially drops but then rises again, followed by a slow roll-off [5]. In these cases, the CCB does detect the island, but it may take longer than 2 seconds to do so. The optimal deployment would likely combine the CCB with other methods such as those described in [4], [6] or [8].

III. Immunity to False Trips During Events

To evaluate the immunity of the CCB to false trips during system level and local events, the CCB has been tested using approximately three years' worth of data collected from a real-world 12.47 kV feeder in the Pacific Northwest. This is a relatively long rural feeder, and thus has relatively high impedance. A 1.7 MW PV plant is installed at the distal end from the substation, and approximately two kilometers upstream from the PV plant is a highly unusual large motor load in which the motors see impulsive use and create a very "spiky" demand on the feeder. The feeder also includes two sets of line regulators, one of which is between the PV plant and the substation. This feeder provides a good platform for testing the false-trip immunity of the CCB.

This feeder was equipped with three PMUs: one reference PMU immediately outside the substation ("PMU1"), and two options for the local PMU, one on the MV side of the PV plant's step-up transformer ("PMU4") and one on the LV side ("PMU5"). The CCB can be run with either local PMU. The CCB was configured with a buffer size of 512 points, a threshold value of 0.7, and a time to trip of zero.

Overall, the CCB performed well in these tests, with the primary factor affecting CCB reliability being reliability of reception of PMU data. Figure 2 shows frequency vs. time for a specific 24-hour period from the data set (May 17, 2014), and Figure 3 shows the correlations between the frequencies measured by PMUs 1 and 4 (blue) and 1 and 5 (red) during the event. The times are in GMT. Just after 6:18 GMT, there was a significant system-level frequency event, which was later determined to be related to the tripping of a large wind farm.

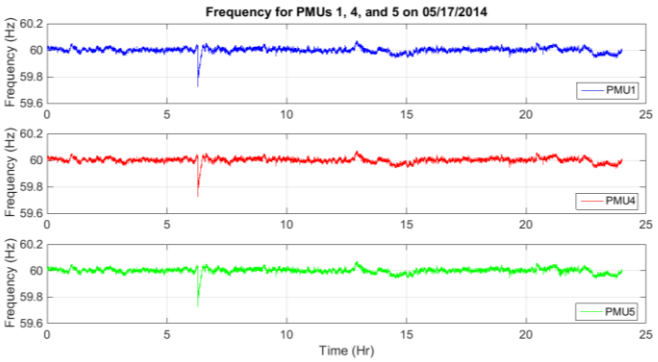

Figure 2. Frequency vs. time for 05/17/2014 as measured by PMUs 1 (blue), 4 (red), and 5 (green).

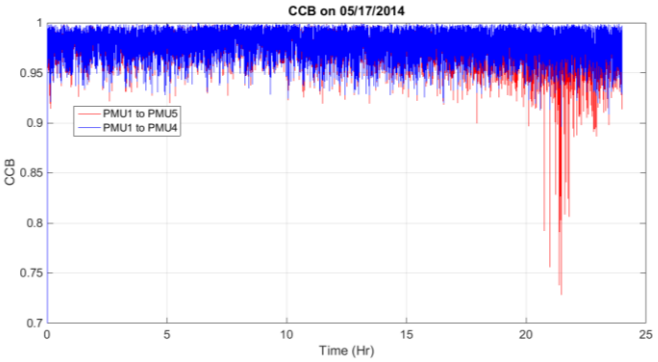

Figure 3. Correlation between PMU 1-4 (blue) and 1-5 (red) frequencies, during the time period shown in Figure 2.

Figure 4 shows a view of Figure 2, zoomed in on the frequency transient caused by this loss of generation event. The frequency drops as low as 59.72 Hz but then shows a well-damped recovery. Figure 5 shows the correlations during the frequency event shown in Figure 4, and indicates that the system-level frequency transient had essentially no impact on the frequency correlation, as expected. Over the entire window shown in Figure 5, the correlation remains above 0.93, and the CCB successfully rides through the event. In fact, it is noted that the correlation actually improves during the event, as the Pearson's r calculation becomes dominated by the frequency variations created by the larger system wide event instead of the local frequency noise.

Figures 6-8 focus on data from later that same day, when Figure 3 indicates that the correlation values dropped very close to the 0.7 threshold value. Figure 6 shows a highly zoomed-in view of the PV plant real and reactive power just before and after one of these events. The moment of the minimum frequency correlation is marked in Figure 6 with a black arrow. Note that there is a large irradiance transient (cloud passage) just before the event, but the cloud passage was not the event trigger. The black arrow indicates a step

change in PV output power that is nearly exactly equal to the output of one of the PV plant's inverters, indicating a single-inverter trip. It can be seen in Figure 6 that the inverter waits for the required 5 minutes, then ramps back up to maximum power.

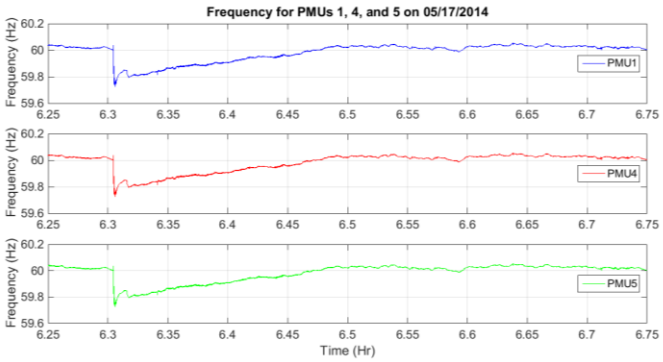

Figure 4. View of Figure 2 zoomed in on the loss-of-generation event just after 6:18 GMT.

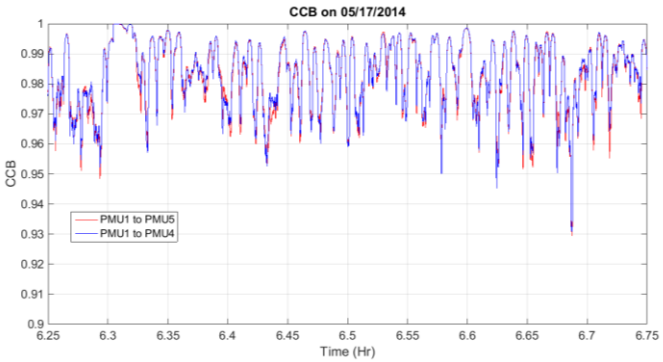

Figure 5. PMU 1-4 (blue) and PMU 1-5 (red) frequency correlations for the data shown in Figure 3.

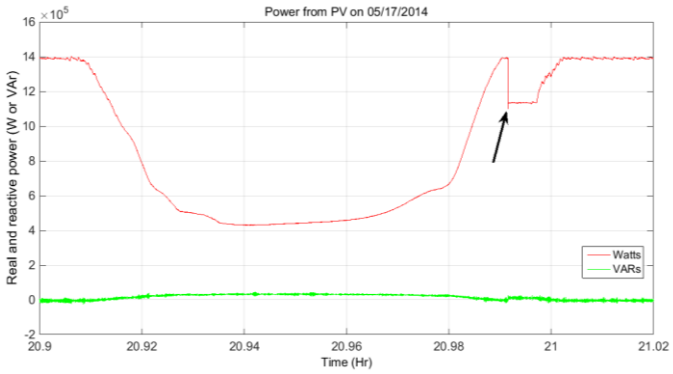

Figure 6. Real (red) and reactive (green) power output from the PV plant during the time period just before and after one of the correlation minima (time point marked with the black arrow).

Figure 7 shows the PMU1 (blue), PMU4 (red), and PMU5 (green) frequency measurements for the same time period as Figure 5. The inverter trips at the spot marked by the black arrows. In each frequency plot, there is a hairline spike in the frequency caused by the phase jump that accompanies the inverter tripping. The magnitude of the spike is much larger in the PMU5 data than in the measurements from the other two PMUs, which is because of the PV step-up transformer's inductive impedance between PMUs 4 and 5. Figure 8 shows the PMU1-4 and PMU1-5 frequency correlations for this same event. The PMU1-PMU5 correlation drops to a minimum of just over 0.75 because of the spike induced by the inverter trip. The PMU1-PMU4 correlation, which is not impacted by the PV transformer impedance, remains above 0.91.

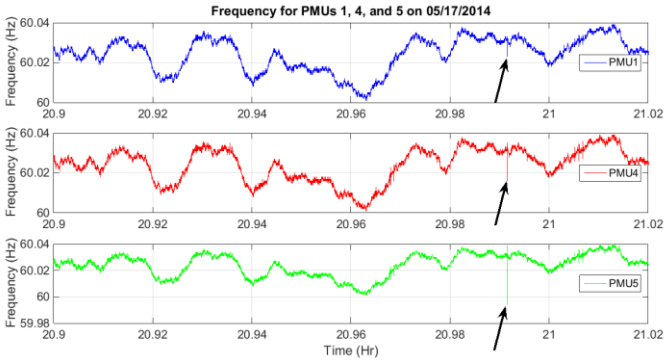

Figure 7. PMU1 (blue), PMU4 (red), and PMU5 (green) frequencies just before and after the marked event in Figure 6.

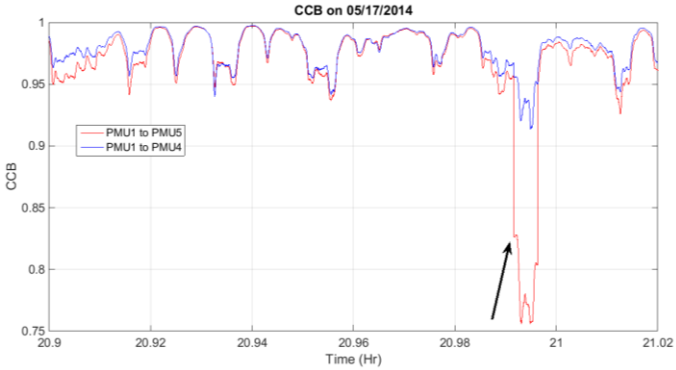

Figure 8. PMU1-PMU4 (blue) and PMU1-PMU5 (red) frequency correlation just before and after the marked event in Figure 5.

Further analysis indicates that all of the sudden drops in correlation seen toward the right of Figure 3 were caused by a series of inverter tripping events over that time period. The CCB does successfully ride through all of them, but reaches a minimum of 0.73, which is definitely lower than desired. The data in Figure 8 suggest that one obvious mitigation scheme may be to place the local PMU on the MV side of the transformer. (The reason for the inverter trips remains unknown at this time.)

IV. Sensitivity to Time Slips

A series of simulations and experiments was conducted in which time slips were added between the local and reference PMU data. This was done for two reasons. The first was to test the robustness of the CCB method in the presence of such time slips. The second was to provide guidance as to whether lower-accuracy timing protocols might be acceptable in future, low-cost distribution-level PMUs for this application. For this test, three different frequency events, a slow, medium, and fast

frequency transient event, were used. These frequency transients were synthesized using a WECC power system model in PSLF. The slow transient is shown in Figure 9, and represents a major loss of generation event. The medium frequency transient shown in Figure 10 was created by simulating an activation of the Chief Joseph Brake. Figure 11 shows the fast transient event, which resulted from a simulated line-to-ground fault on a high-voltage transmission line. The horizontal axes are all in units of seconds.

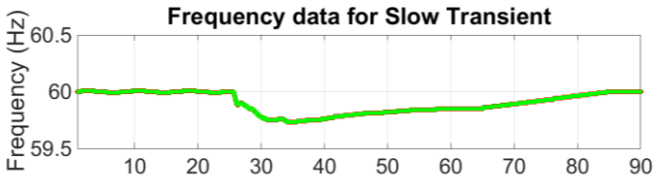

Figure 9. Frequency vs. time during the slow frequency transient.

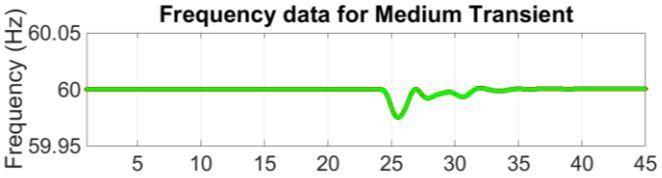

Figure 10. Frequency vs. time during the medium frequency transient.

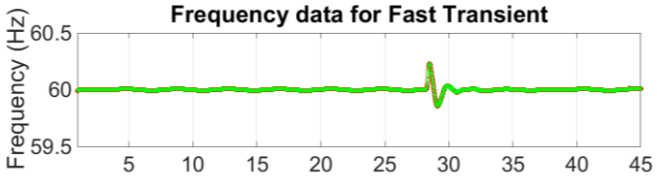

Figure 11. Frequency vs. time during the fast frequency transient.

To evaluate robustness to time slips, all three cases were evaluated in simulation, and the "fast" and "slow" transient events were tested in the laboratory. For the experimental results, the frequency transients were programmed into a grid simulator, and the output of the grid simulator was read by two SEL-751 PMUs that communicated at 60 messages/s (one frequency measurement per line cycle). The PMU frequency measurements were inputs to a CCB algorithm programmed into an SEL-3505 automation controller. Normally, the CCB algorithm in the automation controller time-aligns the samples, but here, a variable time slip was inserted so that the k^{th} local frequency measurement was compared against the $(k+n)^{th}$ remote frequency measurement, where n is zero or any positive integer. The value of n was increased until the CCB indicated a false trip during the frequency transient.

The results are summarized in Table 1. These results indicate that the simulations and experiments matched very well, and also that the CCB tolerates some time slip before it begins to fail to ride through the system-level event. These results suggest that alternate timing protocols, such as the Network Timing Protocol NTPv4, should be feasible alternatives and lower-cost means for signal synchronization, relative to the use of a GPS clock.

Table 1. Sensitivity to time slips of frequency transient test cases.

Case	Cycles of time slip for false trip (simulation)	Cycles of time slip for false trip (experiment)
Slow Transient	9 cycles (150.0 ms)	10 cycles (166.7 ms)
Medium Transient	8 cycles (133.3 ms)	-
Fast Transient	4 cycles (66.7 ms)	4 cycles (66.7 ms)

V. Implications of Electrical Distance

One means for reducing the cost of synchrophasor-based islanding detection is to use a single reference PMU to cover a larger portion of the system via a single reference PMU "heartbeat" broadcast, which could be done inexpensively and reliably via radio. This idea is not new, but thus far little work has been done to explore how large of an area could be covered by a single reference PMU.

It is already known that the reference and local PMUs should be within a single synchronous area. Consider the example two-area system shown in Figure 12. This system contains two synchronous areas connected by three tie lines between buses 5 and 6. Generators 1-4 are all high-inertia generators, Generator 5 is a low-inertia DER representing a synchronous machine in the single-digit MW range, and Generator 6 is a zero-inertia generator representing a PV or Type IV wind plant. The red "X" indicates the location at which a bolted LLLG fault is applied. This fault location was chosen to maximize the frequency transient that results from the fault. Following the fault event, Areas 1 and 2 oscillate or "swing" against each other [10]. During these oscillations, the frequencies between Areas 1 and 2 can become momentarily uncorrelated, which suggests that when applying the CCB, local PMUs in Area 2 should not use a remote PMU signal coming from Area 1. What is less clear is whether the same phenomenon could occur within a single area, if the circuit impedance between the local and remote PMUs becomes sufficiently large.

To test this possibility, the system shown in Figure 12 and the fault at the location of the red "X" was simulated in PSLF with varying circuit impedance between buses 4 and 7. The local PMU is placed on Bus 8, and the remote PMU is at Bus

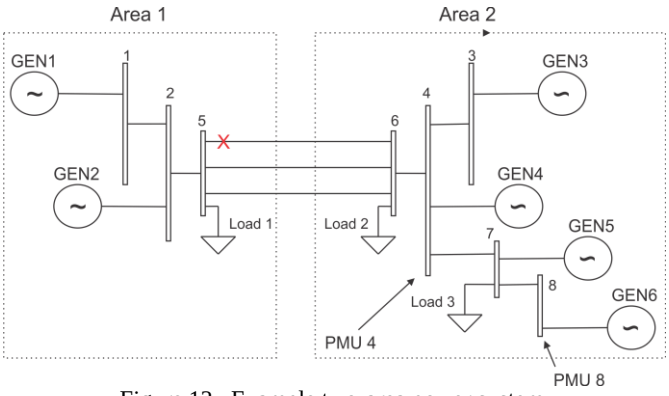

Figure 12. Example two-area power system.

4. The impedance values and the minimum correlation values reached in each case are given in Table 2. No false trip occurs in any case; all five cases ride through successfully.

Figure 13 shows the frequency vs. time and correlation for Case 1. ("Grid Freq" is the remote PMU on Bus 4; "Inv Freq" is the local PMU on Bus 8.) Figure 14 shows the same simulated quantities for Case 5. In Figures 13 and 14, the correlation is zero for the first ~8.5 s as the CCB buffers fill.

Table 2. Definitions of the five impedance cases tested in this section.

Case number	Impedance between buses 4 and 7		Minimum correlation value reached
	R1	X1	
1	0.001	0.02	0.9997
2	0.010	0.10	0.9915
3	0.030	0.25	0.9765
4	0.060	0.50	0.9489
5	0.090	0.85	0.8791

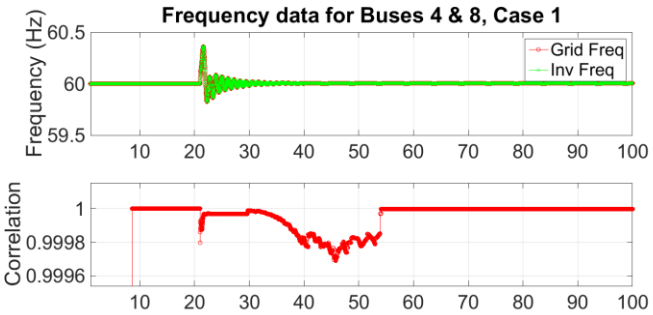

Figure 13. Frequency and correlation vs. time during the fault event on the system in Figure 12, for Case 1.

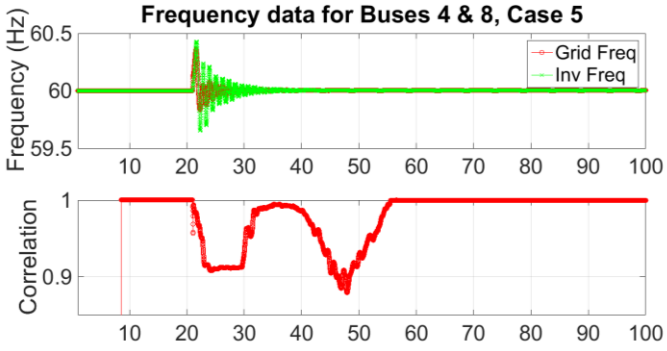

Figure 14. Frequency and correlation vs. time during the fault event on the system in Figure 12, for Case 5.

For Case 1, the correlation is nearly unity for the entire event. In Case 5, the minimum correlation value is about 0.88. In both cases, the minimum correlation value occurs during the very low-amplitude portion of the post-event recovery, and not during the more visible early portion of the frequency transient. In all cases tested, the CCB successfully rides through, suggesting that a single reference PMU could serve all of Area 2 with minimal risk of false trip.

VI. Conclusions

In this paper, three practical issues pertaining to the use of synchrophasors for islanding detection using the correlation coefficient based (CCB) method are discussed: immunity to false trips, sensitivity to time slip, and the effect of "electrical distance" between the local and reference phasor measurement units (PMUs). The results indicate that the CCB has very good immunity to system-level false trips, although it can be susceptible to false tripping for events within the PV plant if the local PMU is on the LV side of the PV plant transformer. The sensitivity to time slips was quantified, and it appears that the CCB could potentially be used with timing protocols with lower accuracy but lower cost than GPS-based methods. Finally, results were presented that suggest that a single reference PMU may be able to cover an entire synchronous operating area, although further work in this area is still needed.

Acknowledgment

This work was supported in part by the U.S. Department of Energy, SunShot Initiative, under award number 25794, and by the Advanced Energy Industries SEGIS-AC grant.

Sandia National Laboratories is a multi-program laboratory managed and operated by Sandia Corporation, a wholly owned subsidiary of Lockheed Martin Corporation, for the U.S. Department of Energy's National Nuclear Security Administration under contract DE-AC04-94AL85000.

References

[1] W. Bower, M. Ropp, "Evaluation of Islanding Detection Methods for Utility-Interactive Inverters in Photovoltaic Systems", Sandia National Laboratories report SAND2002-3591, November 2002.

[2] A. Massoud, K. Ahmed, S. Finney, B. Williams, "Harmonic Distortion-Based Island Detection Technique for Inverter-Based Distributed Generation", *IET Renewable Power Generation* **3**(4), 2009, p. 493-507.

[3] IEEE 1547 Std. 1547-2008, IEEE Standard for Interconnecting Distributed Resources with Electric Power Systems, Institute of Electrical and Electronics Engineers, Inc., New York, NY.

[4] E. Schweitzer, D. Whitehead, G. Zweigle, K. Ravikumar, G. Rzepka, "Synchrophasor-Based Power System Protection and Control Applications", Proceedings of the 2010 International Symposium on Modern Electric Power Systems, September 2010, 10 pgs.

[5] M. Ropp, D. Joshi, M. Mills-Price, S. Hummel, M. Scharf, C Steeprow, M. Osborn, K. Gubba Ravikumar, G. Zweigle, "A Statistically-Based Method of Control of Distributed Photovoltaics Using Synchrophasors", Proceedings of the 2012 IEEE Power and Energy Society General Meeting, July 2012, 7 pgs.

[6] J. Cardenas, G. Mkhael, J. Kaminski, I. Voloh, "Islanding Detection with Phasor Measurement Units", Proceedings of the 2014 Western Protective Relay Conference, October 2014, 13 pgs.

[7] Y. Guo, K. Li, D. Laverty, "A Statistical Process Control Approach for Automatic Anti-Islanding Detection Using Synchrophasors", Proceedings of the 2013 IEEE Power and Energy Society General Meeting, July 2013, 5 pgs.

[8] M. Ropp, S. Perlenfein, D. Joshi, C. Mettler, M. Mills-Price, M. Scharf, K. G. Ravikumar, G. Zweigle, "Synchrophasors for Island Detection", Proceedings of the 38th IEEE Photovoltaic Specialists Conference, June 2012, p. 602-607.

[9] R. Witte, J. Witte, Statistics, 9th ed., pub. 2009 John Wiley and Sons, ISBN 978-0470392225.

[10] F. Saccomanno, Electric Power Systems: Analysis and Control, pub. IEEE Press 2003, ISBN 0471234397.